8000 J. Med. Chem. 2010, 53, 8000–8011
DOI: 10.1021/jm100746q

Journal of Medicinal Chemistry Article

Synthesis and Biological Evaluation of Apogossypolone Derivatives as Pan-active Inhibitors of Antiapoptotic B-Cell Lymphoma/Leukemia-2 (Bcl-2) Family Proteins

Jun Wei, Shinichi Kitada, John L. Stebbins, William Placzek, Dayong Zhai, Bainan Wu, Michele F. Rega, Ziming Zhang, Jason Cellitti, Li Yang, Russell Dahl, John C. Reed, and Maurizio Pellecchia*

Sanford-Burnham Medical Research Institute, 10901 North Torrey Pines Road, La Jolla, California, 92037, United States

Received June 18, 2010

Overexpression of antiapoptotic Bcl-2 family proteins is commonly related with tumor maintenance, progression, and chemoresistance. Inhibition of these antiapoptotic proteins is an attractive approach for cancer therapy. Guided by nuclear magnetic resonance (NMR) binding assays, a series of 5,5′ substituted compound **6a** (Apogossypolone) derivatives was synthesized and identified pan-active antagonists of antiapoptotic Bcl-2 family proteins, with binding potency in the low micromolar to nanomolar range. Compound **6f** inhibits the binding of BH3 peptides to Bcl-X_L, Bcl-2, and Mcl-1 with IC_{50} values of 3.10, 3.12, and 2.05 μM, respectively. In a cellular assay, **6f** potently inhibits cell growth in several human cancer cell lines in a dose-dependent manner. Compound **6f** further displays in vivo efficacy in transgenic mice and demonstrated superior single-agent antitumor efficacy in a PPC-1 mouse xenograft model. Together with its negligible toxicity, compound **6f** represents a promising drug lead for the development of novel apoptosis-based therapies for cancer.

Introduction

For the maintenance of normal tissue homeostasis, ensuring a proper balance of cell production and cell loss, cells undergo a process known as apoptosis or programmed cell death.[1,2] Defective apoptosis contributes to tumorgenesis and chemoresistance.[3,4] Central regulators of this process are the B-cell lymphoma/leukemia-2 (Bcl-2[a]) family proteins.[5−7] To date, six antiapoptotic members of the Bcl-2 family have been identified and characterized in human, including Bcl-2, Bcl-X_L, Mcl-1, Bfl-1, Bcl-W, and Bcl-B. Both X-ray crystallography and NMR spectroscopy structural characterizations of several of these proteins have identified a heterodimerization interface composed of an hydrophobic crevice on the surface of antiapoptotic Bcl-2 family proteins and the BH3 dimerization domain of pro-apoptotic family members.[8] Hence, small molecules that bind in the hydrophobic crevide of anto-apoptotic Bcl-2 protein would mimic the BH3 domain of pro-apoptotic proteins, presumably inducing apoptosis and/or abrogating the ability of antiapoptotic Bcl-2 proteins to inhibit cancer cell death.[8−11]

We and others have reported that the natural product **1** (Gossypol) (Figure 1A) is a potent inhibitor of Bcl-2, Bcl-X_L, and Mcl-1, functioning as a BH3 mimic.[12−16] The (−) atropisomer of compound **1** (AT101, Ascenta Pharmaceuticals) is currently in phase II clinical trials, displaying single-agent antitumor activity in patients with advanced malignancies.[15−17] Given that compound **1** may target other proteins due to two reactive aldehyde groups, we designed compound **2a** (Apogossypol) (Figure 1A), a compound that lacks these aldehydes but retains activity against antiapoptotic Bcl-2 family proteins in vitro.[18] Recently, we further compared the efficacy and toxicity in mice of compounds **1** and **2a**, and our preclinical in vivo data show that compound **2a** has superior efficacy and markedly reduced toxicity compared to **1**.[19] Moreover, we evaluated of the single-dose pharmacokinetic characteristics of **2a** in mice, and compound **2a** displayed superior blood concentrations over time compared to compound **1** due to slower clearance.[20] Recently, we reported the separation and characterization of atropoisomers of **2a**,[21] and these studies revealed that the racemic **2a** is as effective as its individual isomers.[21] We further reported the synthesis and evaluation of 5,5′ alkyl, ketone, and amide substituted **2a** derivatives, with the best compounds **3a** (BI79D10)[22] and **4a** (8r)[23] displaying improved in vitro and in vivo efficacy compared to **2a** (Figure 1A), and of the optically pure compound **9** (BI97C1) (Supporting Information Figure 1A),[24] with marked efficacy in vivo.[24]

Compound **5** (Gossypolone), a major metabolite of compound **1** formed by oxidation, displayed similar cytotoxic effects as compound **1** on several cancer cell lines (Figure 1B)

*To whom correspondence should be addressed. Phone: (858) 6463159. Fax: (858) 7955225. E-mail: mpellecchia@sanfordburnham.org.

[a] Abbreviations: Bcl-2, B-cell lymphoma/leukemia-2; EDCI, 1-ethyl-3-(3′-dimethylaminopropyl)carbodiimide; 1D-^{1}H NMR, one-dimensional ^{1}H nuclear magnetic resonance spectroscopy; SAR, structure−activity relationship; FPA, fluorescence polarization assays; ITC, isothermal titration calorimetry; CLL, chronic lymphocytic leukemia; WT, wild type; MEFs, mouse embryonic fibroblast cells; DKO, Bax/Bak double knockout; DKO/MEFs, Bax/Bak double knockout mouse embryonic fibroblast cells; ACN, acetonitrile; LC-MS, liquid chromatography and tandem mass spectrometry; HPLC, high-performance liquid chromatography; TROSY, transverse relaxation-optimized spectroscopy; ADME, absorption, distribution, metabolism, and excretion; DMSO, dimethyl sulphoxide; PPC-1, human prostatic cancer cell line; PAMPA, parallel artificial membrane permeation assay; FITC, fluorescein isothiocyanate; GST, glutathione-S-transferase; PBS, phosphate-buffered saline; SE, standard error; PI, propidium iodide; NADPH, nicotinamide adenine dinucleotide phosphate; rpm, rotations per minute; AUC, area under the curve.

 Published on Web 10/29/2010

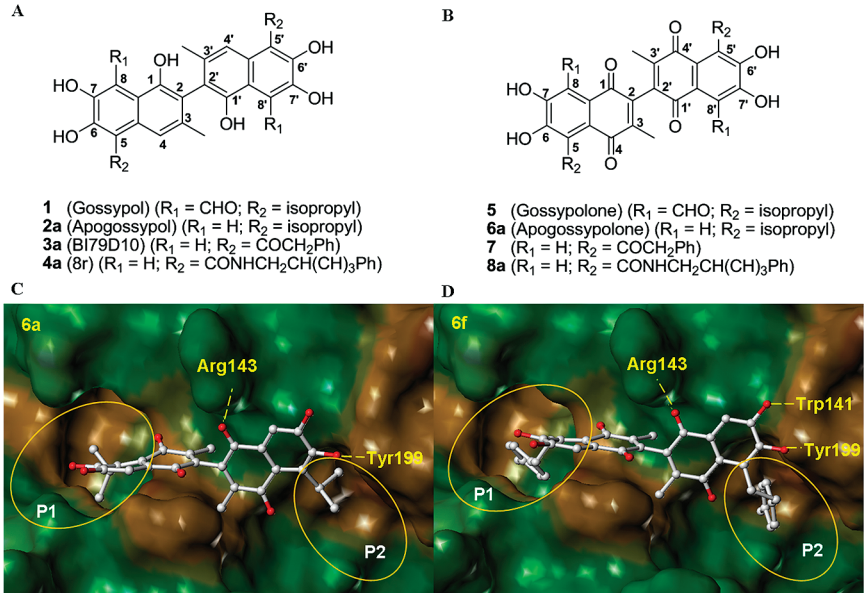

Figure 1. (A) Structure of compounds **1**, **2a**, **3a**, and **4a**. (B) Structure of compounds **5**, **6a**, **7**, and **8a**. Molecular docking studies. Docked structures of (C) compound **6a** and (D) compound **6f** into Bcl-2 (PDB: 1YSW).

and has been recently proposed for treatment of cancer.[25,26] Compound **6a** (Apogossypolone) a derivative of **5**, has as well been reported as a potent inhibitor of Mcl-1 and Bcl-2 proteins.[27−32] Compound **6a** blocks binding of Bim and Bcl-2 and induced apoptosis in a number of human cancer cell lines (Figure 1B).[27−32] Compound **6a** also induced regression in several tumor xenograft models and its maximum tolerated dose (MTD) when administered orally is above 240 mg/kg while the MTD of (−) **1** is 50 mg/kg.[27,31,32] It is therefore attractive to further explore whether **6a** derivatives displayed similar or improved biological activities compared to **6a**. In fact, we have previously demonstrated that certain 5,5′ substituted **2a** derivatives (**3a** and **4a**) displayed improved in vitro and in vivo activities compared to **2a**.[22,23] Therefore, we envision that 5,5′ substitution of **6a** could result in compounds with improved biological activities. Hence, we report on the synthesis and biological evaluation of novel 5,5′ substituted **6a** derivatives (**6**−**8**), which replace the isopropyl groups of **6a** with various alkyl (**6**), ketone (**7**), and amide (**8**) groups at 5,5′ positions (Figure 1B).

Results and Discussion

Compound **6a** has recently been reported as an inhibitor of Bcl-X_L, Bcl-2, and Mcl-1.[26−28] Molecular docking studies of compound **6a** into the BH3 binding groove in Bcl-2[33,34] (Figure 1C) suggest that **6a** forms two hydrogen bonds with residues Arg 143 and Tyr 199 in Bcl-2 through the 1′ oxygen and 6′ hydroxyl groups, respectively. The isopropyl group on the left naphthalene ring inserts into the first hydrophobic pocket (P1) in Bcl-2 (Figure 1C), while the isopropyl group on the right naphthalene ring inserts into the hydrophobic pocket (P2) (Figure 1C). Analysis of the predicted binding models indicates that while the overall core structure of compound **6a** fits very well into BH3 binding groove of Bcl-2, the two isopropyl groups do not fully occupy the hydrophobic pockets P1 and P2. Therefore, a library of 5,5′ substituted **6a** derivatives (Figure 1B) that replace the isopropyl groups with suitable substituents was designed with the aim of deriving novel molecules that could occupy the hydrophobic pockets on Bcl-2 and other members of this protein family more efficiently.

Synthetic routes (Schemes 1−2) were developed to install a variety of groups at 5,5′ position, and synthesis of **6a** and its 5,5′ amide substituted derivatives are outlined in Scheme 1. Compound **1** was treated with NaOH solution at 90 °C to provide compound **2a**, which was readily methylated in the presence of potassium carbonate to afford compound **9** (Scheme 1). Compound **9** was oxidized to compound **10** using periodic acid.[35] Subsequent demethylation of the compound **10** using boron tribromide afforded compound **6a**. Reaction of compound **9** with $TiCl_4$ followed by dichloromethyl methyl ether resulted in loss of isopropyl groups and simultaneous bisformylation to give aldehyde compound **11**.[36] The aldehyde groups of compound **11** were oxidized and coupled with a variety of commercially available amines in the presence of 1-ethyl-3-(3′-dimethylaminopropyl)carbodiimide (EDCI) to afford amide compound **12**. Subsequent demethylation of compound **12** afforded compound **4**.[37,38] Several oxidation reagents such as [bis(trifluoroacetoxy)iodo]benzene,[39] potassium nitrosodisulfonate,[40] and ferric chloride[41] were used to converted phenol **4** to quinone **8**, and the ferric chloride is the most efficient oxidation reagent for this conversion in our hand (Scheme 1).

The synthesis of 5,5′ alkyl substituted **6a** derivatives were outlined in Scheme 2. Compound **11** was treated with different Grignard or lithium reagents to afford a secondary alcohol **13**, which was oxidized to give the phenone **14** by pyridinium chlorochromate. Alcohol **13** and phenone **14** were readily reduced using triethylsilane to afford alkyl compound **15**.[42] Compound **15** was then demethylated using boron tribromide to afford compound **2** (Scheme 2). Oxidation of compound **2** using ferric chloride gave **6** as 5,5′ alkyl substituted **6a** derivatives. The reduction of ketone **3** using H_2 in the presence of Pd/C also afforded compound **2**.[43] Demethylation of compound **14**[22] followed by ferric chloride oxidation afforded compound **7** as a 5,5′ ketone substituted **6a** derivative (Scheme 2).

The synthesized 5,5′ substituted **6a** derivatives were first screened by one-dimensional ^{1}H nuclear magnetic resonance spectroscopy (1D ^{1}H NMR) binding assays against Bcl-X_L, as

Scheme 1[a]

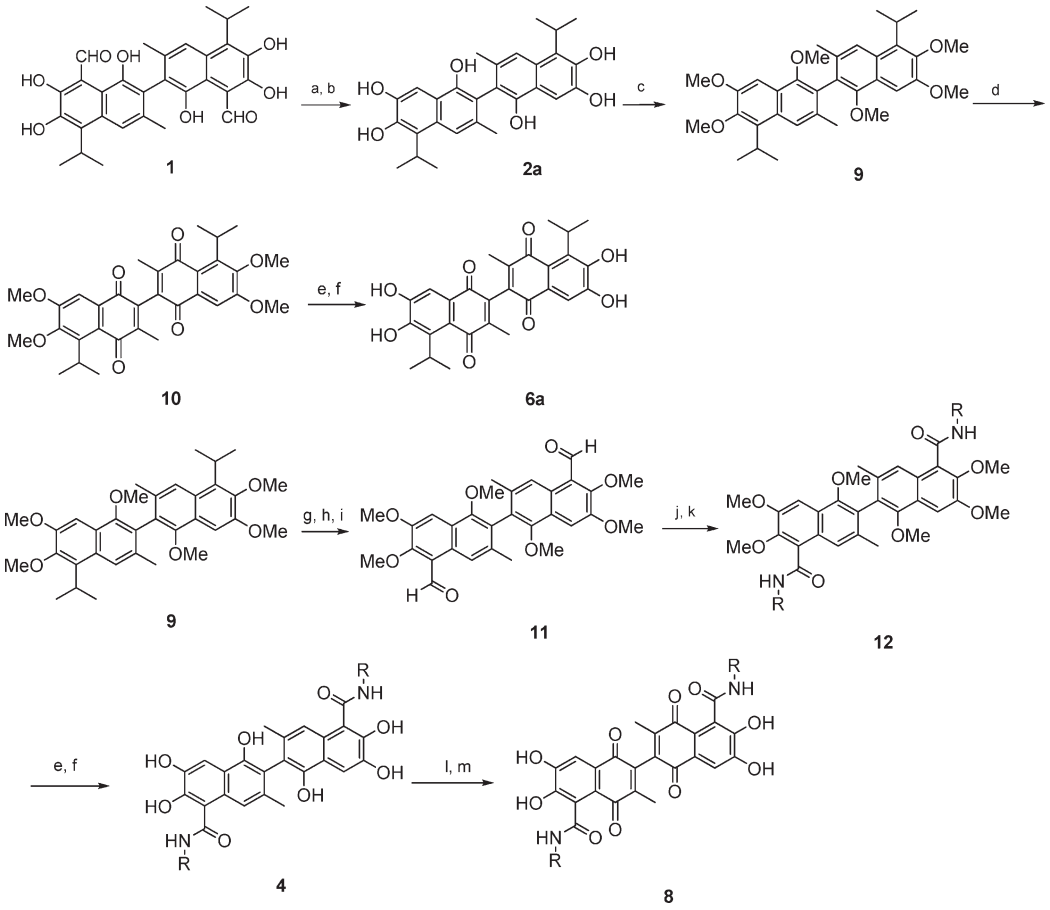

[a] Reagents and conditions: (a) NaOH, H_2O, reflux; (b) H_2SO_4; (c) DMS, K_2CO_3; (d) H_5IO_6, 95 °C; (e) BBr_3, CH_2Cl_2; (f) HCl, H_2O; (g) $TiCl_4$, rt; (h) Cl_2CHOCH_3, rt; (i) HCl, H_2O; (j) $NaClO_2$, H_2O_2, KH_2PO_4, CH_3CN, rt; (k) EDCI, NH_2R, HOBT, rt; (l) $FeCl_3$, CH_3COOH, 60 °C; (m) 20% H_2SO_4.

Scheme 2[a]

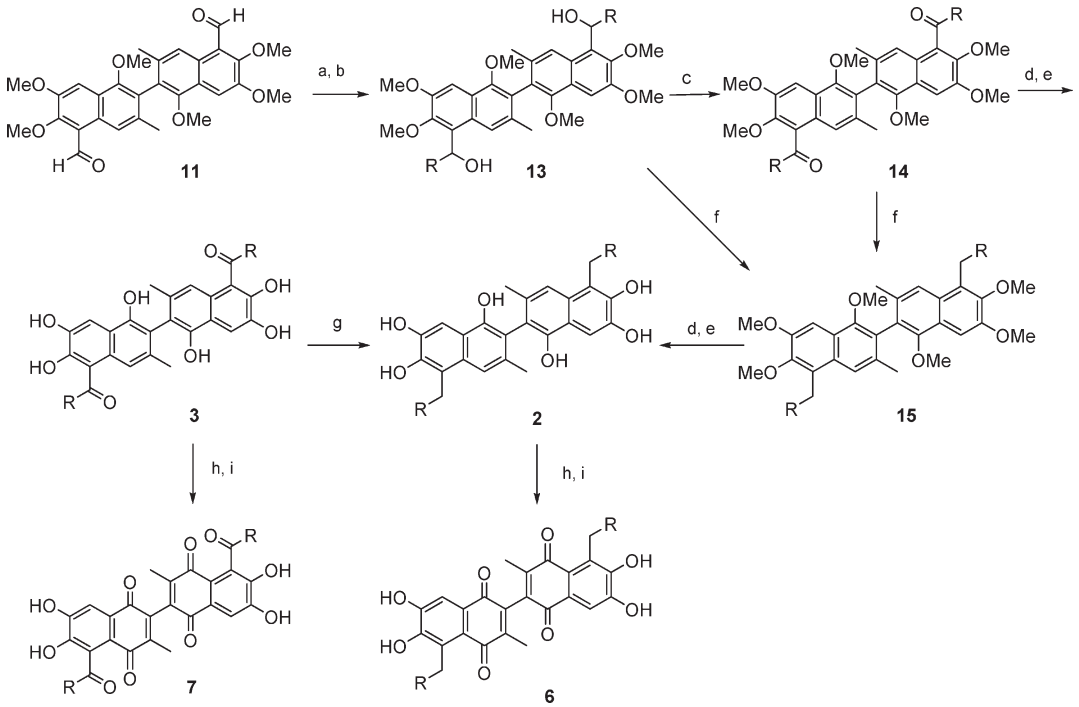

[a] Reagents and conditions: (a) RMgBr or RLi, rt; (b) NH_4Cl, H_2O; (c) pyridinium chlorochromate, CH_2Cl_2, rt; (d) BBr_3; (e) HCl, H_2O; (f) Et_3SiH, TFA; (g) Pd/C, H_2, CH_3COOH; (h) $FeCl_3$, CH_3COOH, 60 °C; (i) 20% H_2SO_4.

Table 1. Evaluation of 5,5′ Substituted **6a** Derivatives Using a Combination of 1D ^{1}H-NMR Binding Assays and Cell Viability Assays

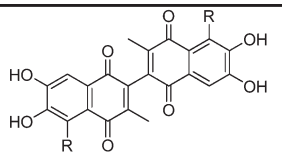			EC_{50} (μM)				
Compound	**R =**	**1D-^{1}H NMR** *a**	**PC3** *b** **(μM)**	**H460** *b** **(μM)**	**H1299** *b** **(μM)**	**BP3** *c** **(μM)**	**RS4;11** *c** **(μM)**
6a		+++	**1.46 ± 0.33**	**0.40 ± 0.07**	**2.76 ± 0.72**	**11.73 ± 2.15**	**7.47 ± 2.78**
8a	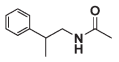	+++	**7.6 ± 1.41**	**5.75 ± 1.34**	**>30**	**12.9 ± 1.91**	**>30**
8b		+++	**5.44 ± 0.34**	**6.16 ± 1.48**	**>30**	**21.64 ± 0.85**	**>30**
8c	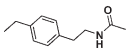	+++	**7.70 ± 0.64**	**4.40 ± 0.70**	**9.10 ± 5.20**	**22.23 ± 1.43**	**>30**
7		+++	**5.44 ± 0.24**	**7.38 ± 1.07**	**>30**	**9.58 ± 4.16**	**>30**
6b		+++	**8.50 ± 2.89**	**0.73 ± 0.29**	**10.64 ± 5.02**	**10.93 ± 0.43**	**11.72 ± 0.68**
6c		+	**5.50 ± 0.74**	**0.70 ± 0.34**	**2.32 ± 0.51**	**12.84 ± 1.16**	**9.83 ± 0.26**
6d		+	**2.40 ± 0.24**	**2.20 ± 0.76**	**1.32 ± 0.30**	**15.61 ± 0.10**	**15.43 ± 1.86**
6e		++	**1.40 ± 0.14**	**1.04 ± 0.13**	**0.85 ± 0.36**	**8.72 ± 2.53**	**4.75 ± 0.01**
6f		++	**1.10 ± 0.08**	**0.59 ± 0.06**	**1.56 ± 0.17**	**4.18 ± 0.50**	**3.08 ± 0.59**
6g		++	**1.30 ± 0.18**	**0.92 ± 0.09**	**1.53 ± 0.41**	**6.0 ± 0.10**	**3.83 ± 0.70**
6h		++	**2.00 ± 0.17**	**1.62 ± 0.16**	**2.16 ± 0.27**	**30.0 ± 2.40**	**15.0 ± 0.24**
6i		+++	**0.59 ± 0.22**	**0.13 ± 0.08**	**0.31 ± 0.19**	**10.1 ± 0.04**	**6.9 ± 1.76**
6j	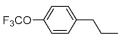	+	**8.99 ± 2.49**	**1.44 ± 0.20**	**2.38 ± 0.21**	**16.12 ± 0.07**	**7.32 ± 0.90**
6k	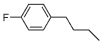	+	**2.62 ± 0.31**	**1.48 ± 0.02**	**1.91 ± 0.17**	**14.61 ± 0.06**	**11.25 ± 0.54**
6l		+++	**0.21 ± 0.05**	**0.19 ± 0.04**	**2.99 ± 1.21**	**0.48 ± 0.01**	**1.13 ± 0.60**
6m		+++	**2.97 ± 0.98**	**0.98 ± 0.15**	**10.30 ± 3.84**	**0.81 ± 0.06**	**1.74 ± 0.11**

a *Four-point-rating scale: +++, very active; ++, active; +, mild; −, weak. *b* *Compounds against cell line using ATP-LITE assay. *c* *Compounds against cell line using Annexin V-FITC and propidium iodide assay.

we reported previously (Table 1 and Supporting Information Figure 1B).[44] A group of compounds (**6a**, **6b**, **6f**, **6i, 6l**, **6m**, **7**, **8a**−**c**) induced chemical shift changes in active site methyl groups (region between −0.38 and 0.42 ppm) in the one-dimensional

Table 2. Cross-Activity of Selected 5,5′ Substituted **6a** Derivatives against Bcl-X_L, Bcl-2, Mcl-1, and Bfl-1

	IC_{50} (μM) FPA				K_d (μM) ITC
compd	Bcl-X_L	Bcl-2	Bfl-1	Mcl-1	Bcl-X_L
6a	0.63 ± 0.02	0.37 ± 0.02	2.17 ± 0.35	0.54 ± 0.03	2.80 ± 0.60
6b	0.55 ± 0.06	0.25 ± 0.02	1.41 ± 0.11	0.47 ± 0.03	1.50 ± 0.80
6f	3.10 ± 0.28	3.12 ± 0.15	14.7 ± 6.63	2.05 ± 0.15	2.50 ± 2.20
6i	0.34 ± 0.03	0.29 ± 0.01	0.65 ± 0.05	0.24 ± 0.02	0.45 ± 0.26
6c	2.99 ± 0.16	2.27 ± 0.15	ND[a]	3.08 ± 0.17	ND
6d	12.65 ± 4.34	6.73 ± 2.24	ND	5.90 ± 0.54	ND
6e	1.79 ± 0.14	2.57 ± 0.12	9.72 ± 1.38	1.29 ± 0.05	ND
6g	1.44 ± 0.06	2.17 ± 0.14	5.27 ± 0.76	0.67 ± 0.03	ND
6l	0.15 ± 0.06	0.34 ± 0.06	0.70 ± 0.07	0.40 ± 0.05	ND
7	0.34 ± 0.02	0.22 ± 0.02	0.69 ± 0.03	0.35 ± 0.02	ND
8a	0.32 ± 0.01	0.23 ± 0.01	0.71 ± 0.06	0.47 ± 0.03	ND
8c	0.24 ± 0.02	0.21 ± 0.01	1.25 ± 0.09	0.32 ± 0.02	ND

[a] ND = not determined.

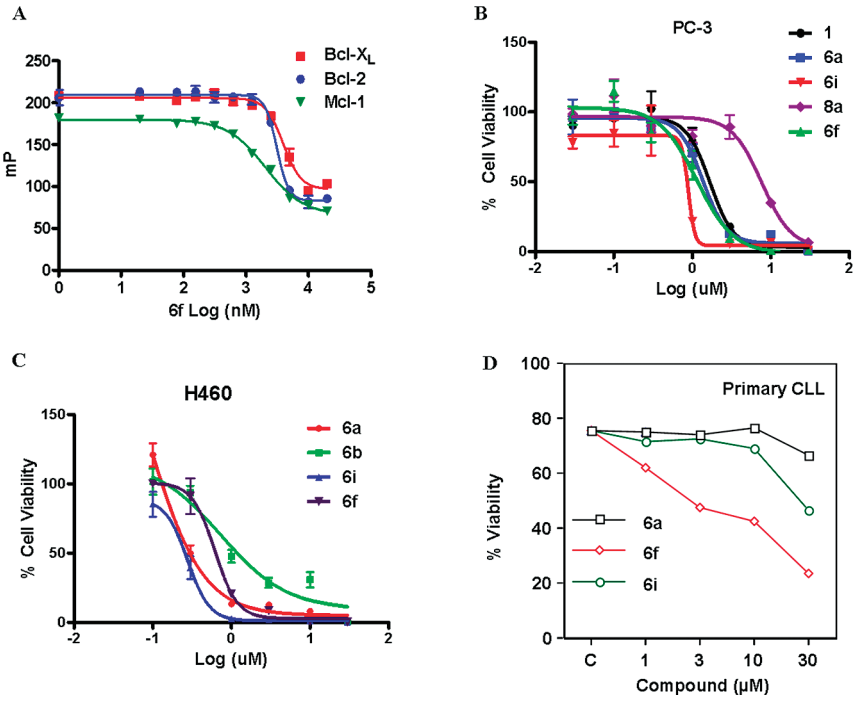

Figure 2. (A) Fluorescence polarization-based competitive curves of **6f** using Bcl-X_L (red square), Bcl-2 (blue dot), and Mcl-1 (green downward pointing triangle). (B) Inhibition of cell growth by compounds **1** (dark dot), **6a** (blue square), **6i** (red downward pointing triangle), **8a** (purple diamond), and **6f** (green upward pointing triangle) in the PC-3 human prostate cancer cell line. Cells were treated for three days and cell viability was evaluated using ATP-LITE assay. (C) Inhibition of cell growth by compounds **6a** (red dot), **6b** (green square), **6i** (blue upward pointing triangle), and **6f** (purple downward pointing triangle) in the H460 human lung cancer cell line. Cells were treated for three days, and cell viability was evaluated using ATP-LITE assay. (D) Inhibition of cell growth by compounds **6a** (dark square), **6f** (red diamond), and **6i** (green circle) in the human primary CLL cells. Cells were treated for 1 day, and cell viability was evaluated using Annexin-V apoptosis assay.

^{1}H NMR spectra of Bcl-X_L (Table 1). To confirm the result from the 1D ^{1}H NMR binding assay, we also produced uniformly ^{15}N-labeled Bcl-X_L protein and measured 2D [^{15}N, ^{1}H]-HSQC correlation spectra in the absence and presence of selected compounds. Consistent with 1D ^{1}H NMR binding assays, compounds **6f**, **6i**, and **8a** displayed strong binding to Bcl-X_L, as qualitatively evaluated by the nature of the shifts at the ligand/protein ratio of 1:1 (Supporting Information Figure 1C−D). To confirm the results of the NMR binding data, we further evaluated the binding affinity of selected compounds for Bcl-X_L using FP assay (Table 2). In agreement with NMR binding, compound **6f** displayed potent binding affinity to Bcl-X_L with an IC_{50} value of 3.1 μM in FP assay (Table 2 and Figure 2A). A group of compounds (**6a**, **6b**, **6i**, **6l**, **6m**, **7**, **8a**, **8c**) were 5−19 times more potent than **6f**, with IC_{50} values ranging from 0.16 to 0.63 μM in the same assay (Table 2 and Supporting Information Figure 2A−B).

To further confirm results of the NMR binding data and the FP assays, we also evaluated the binding affinity of selected compounds (**6a**, **6b**, **6f**, **6i**) for Bcl-X_L using isothermal titration calorimetry (ITC) (Table 2). In agreement with NMR binding and FPA data, compound **6f** displayed high binding affinity to Bcl-X_L, with a K_d value of 2.5 μM by ITC, and compound **6i** showed increased binding affinity, with a K_d value of 0.45 μM in same assay. Compound **6a** showed similar binding affinity with **6f**, with a K_d value of 2.80 μM by ITC. Consistent with the NMR binding, FPA, and ITC data, compounds **6a**, **6d**−**6g**, **6i**, and **6l** displayed potent efficacy in inhibiting cell growth in a three-day ATP-Lite assay in the PC3 cell line, which expresses high levels of Bcl-X_L

Table 3. Plasma Stability, Microsomal Stability and Membrane Permeability of Selected 5,5′ Substituted **6a** Derivatives

compd	plasma stability (T = 40 min) (%)	microsomal stability (T = 40 min) (%)	membrane permeability (PAMPA, LogPe)
6a	77	47	-5.94 ± 0.09
8a	91	71	-7.88 ± 0.08
6b	98	69	-6.17 ± 0.02
6d	74	98	-5.82 ± 0.20
6e	81	89	-6.58 ± 0.05
6f	86	63	-5.59 ± 0.08
6g	87	88	-6.65 ± 0.05
6i	95	91	-7.11 ± 0.04

(Table 1 and Figure 2B). The average EC_{50} value of **6i** and **6l** is 0.40 μM, hence 3.5-fold more potent than **6a** (EC_{50} = 1.5 μM) (Figure 2B). Compound **6f** (EC_{50} = 1.1 μM) displayed similar efficacy in inhibiting PC3 cell growth as the potent compound **6a** in same assay (Table 1). However, although compounds **8a** and **8c** displayed strong binding affinity to Bcl-X_L in the NMR binding assay and FP assay, they showed relatively weaker efficacy in inhibiting growth of PC3 cells, with EC_{50} values around 7.6 μM (Table 1). The discrepancy is likely due to high hydrophilicity and molecular weight of **8a** and **8c** which may result in low cell permeability. Cell permeability of selected compounds was therefore evaluated using the parallel artificial membrane permeability assay (PAMPA) (Table 3). As anticipated, compounds **8a** has a lower LogPe value of −7.9, indicating poor cell membrane permeability, while the LogPe value of **6f** is −5.6, indicating excellent cell membrane permeability. Compared to **6f**, compound **6a** also has relatively lower cell membrane permeability (LogPe = −5.9).

In addition to Bcl-X_L, other members of the Bcl-2 family are known to play critical roles in tumor survival.[45,46] Therefore, we further evaluated the binding properties and specificity of selected 5,5′ substituted **6a** derivatives against Bcl-2, Mcl-1 and Bfl-1 using FP assays (Table 2 and Supporting Information Figure 2B). Compound **6f** displayed potent affinity against Bcl-2 (IC_{50} = 3.12 μM) and Mcl-1 (IC_{50} = 2.05 μM) and relatively lower affinity against Bfl-1 (IC_{50} = 14.0 μM) in FP assays (Table 2). Compound **6f** was further evaluated against H460 and H1299 cancer cell lines, which express high levels of Bcl-2 and Mcl-1, respectively (Table 1).[46−48] Consistent with FPA data, compound **6f** displayed potent efficacy in inhibiting cell growth in H460 and H1299 cell lines in a three-day ATP-Lite assay, with EC_{50} values of 0.59 and 1.5 μM, respectively, which is comparable with **6a** (Table 1 and Figure 2C). Molecular docking studies of compound **6f** demonstrated that 1-methyl-4-propylbenzene groups at 5,5′ positions inserted deeper into hydrophobic pockets (P1 and P2) in Bcl-2 (Figure 1D). On the basis of the docking models, compound **6f** also forms two hydrogen bonds with residues Arg 143 and Tyr 199 in Bcl-2 through the 1′ oxygen and 6′ hydroxyl groups, respectively. In addition, the 7′ hydroxyl group on the right naphthalene ring also formed an additional hydrogen bond with residue Tyr141 (Figure 1D). Other 5,5′ substituted **6a** derivatives, such as **6b**, **6i**, and **6l** also displayed strong pan-active inhibitory properties against Bcl-2, Mcl-1, and Bfl-1. The most potent compound **6i** displaces BH3 binding to Bcl-2, Mcl-1, and Bfl-1, with IC_{50} values of 0.29, 0.24, and 0.65 μM (Table 2 and Supporting Information Figure 2B), respectively, in FP assays. In agreement with these FPA results, the compound **6i** showed potent cell growth inhibitory activity against the H460 and H1299 cell lines in a three-day ATP-Lite assay, with IC_{50} values of 0.13 and 0.31 μM, respectively (Table 1 and Figure 2C). The H460 cell line has been studied by several groups with respect to sensitivity to Bcl-2 antagonists.[47−49] However, although compounds **7**, **8a**, and **8c** display potent binding affinity to Bcl-2 and Mcl-1, with average IC_{50} values of 0.22 and 0.38 μM, respectively, in FP assays, they showed relative weak efficacy in inhibiting growth of H460 and H1299 cells, with average EC_{50} values of around 5.8 and 17 μM, respectively (Table 1). This discrepancy is partially due to high hydrophilicity and molecular weight of 5,5′ substituted ketone and amide **6a** derivatives, resulting in reduced cell permeability.

We evaluated the ability of 5,5′ substituted **6a** derivatives to induce apoptosis of the human leukemia RS4;11 cell line (which expresses high levels of Bcl-2 and Bcl-X_L) and human lymphoma BP3 cell line (which express high levels of Bfl-1 and Mcl-1) in one-day Annexin-V apoptosis assay. For this assay, we used Annexin V-FITC and propidium iodide (PI) double staining, followed by flow-cytometry analysis (Table 1). The pan-Bcl-2 family inhibitor **6f** effectively induced apoptosis of the RS4;11 and BP3 cell lines in a dose-dependent manner (Table 1 and Supporting Information Figure 2C), with EC_{50} values of 3.5 and 3.0 μM, respectively, which are 2−3 times more potent than **6a** (EC_{50} values of 7.4 and 9.2 μM, respectively) in the same assays (Table 1 and Supporting Information Figure 2D). By comparison, the potent Bcl-X_L and Bcl-2 antagonist compound **10** (ABT-737)[33] displayed no cytotoxic activity against BP3 cell lines, presumably because compound **10** is not effective against Mcl-1 and Bfl-1.[23,33,45,50] Consistent with previous results obtained for human PC3, H460 and H1299 cancer cell lines, most of synthesized **6a** derivatives induced apoptosis of the RS4;11 and BP3 cell lines in a dose-dependent manner (Table 1 and Supporting Information Figure 2D).

To further explore the anticancer activities of selected 5,5′ substituted **6a** derivatives, we tested their ability to induce apoptosis of primary lymphocytic leukemia cells freshly isolated from different patients affected by chronic lymphocytic leukemia (CLL) in a one-day Annexin-V apoptosis assay (Figure 2D and Supporting Information Figure 3A−B). Consistent with previous results obtained for human RS4;11 and BP3 cell lines, the most potent compound **6f** effectively induced apoptosis of two primary CLL samples (Figure 2D and Supporting Information 3B) in a dose-dependent manner, with LD_{50} values of 10 and 15 μM, respectively. By comparison, compound **6a** display weak activities in these two primary cells (LD_{50} > 30 μM). Compound **6f** was further tested against primary leukemic cells freshly isolated from different six patients affected by CLL using the same assay. In agreement with previous CLL results, compound **6f** effectively induced apoptosis of all six CLL samples, with LD_{50} values ranging from 1.0 to 16.9 μM (Supporting Information Table 1). Compound **6c** also effectively induced apoptosis of primary CLL samples, with a LD_{50} value of 6.5 μM, while **6a** is less effective (LD_{50} > 30 μM) (Supporting Information Figure 3A).

To test the pharmacological properties of 5,5′ substituted compound **6a** derivatives, we determined their in vitro plasma stability, microsomal stability, and cell membrane permeability (Table 3). From these studies, we could conclude that most of our synthesized compounds displayed superior plasma and microsomal stability compared to **6a** (Table 3). Compounds **6f** and **6i** degraded 37% and 9%, respectively, after 1 h incubation in rat plasma, while **6a** degraded 53% under the same conditions. In addition, compounds **6f** and **6i** also displayed

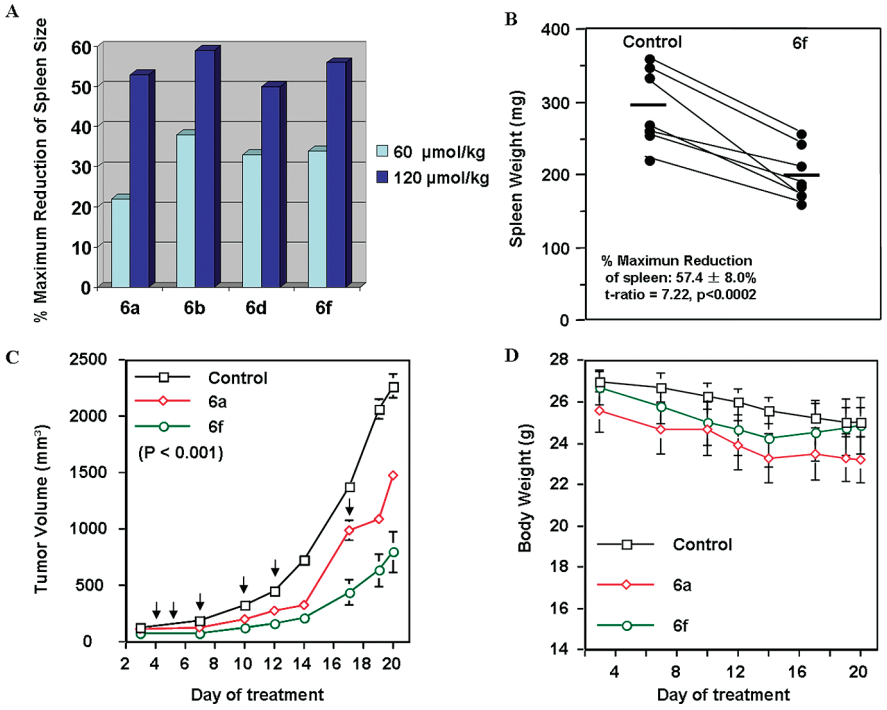

Figure 3. Characterization of compounds in vivo. (A) Effects of 5,5′ substituted **6a** derivatives on shrinkage of Bcl-2 mouse spleen at a single intraperitoneal injection dose of 60 μmol/kg and 120 μmol/kg, respectively. All shrinkage data are percentage of maximum reduction of mice spleen size. (B) Effects of compound **6f** at 60 μmol/kg on reduction of spleen weight of six Bcl-2 mice treatment with a single intraperitoneal injection. Data shown as means ± SE (n = 7). $P < 0.0002$. (C) Effect of ip **6f** and **6a** at 50 mg/kg on the growth of PCC-1 tumors in nude mice. Compound **6f** significantly inhibited tumor growth compared to vehicle control determined with Anova statistics ($P < 0.001$). Tumor growth inhibition ratios (T/C %) were calculated by dividing the average tumor volume in the treatment group by the average tumor volume in the control group. Dark down arrow "↓" represents the date mice were treated with compounds (D) Average body weight changes during treatment.

better plasma stability and only degraded by 14% and 5%, respectively, after 1 h incubation in rat plasma preparations, while **6a** degraded 23% under the same conditions.

Hence, using a combination of 1D ^{1}H NMR binding assays, FP assays, ITC, cytotoxicity assays, and preliminary in vitro ADME data, we selected compounds for in vivo studies using a B6-Bcl-2 transgenic mouse model. B-cells of the B6 transgenic mice overexpress human Bcl-2 and accumulate in the spleen of mice. The spleen weight is used as an end point for assessing in vivo activity, as we have determined that the spleen weight is highly consistent in age- and sex-matched Bcl-2-transgenic mice, varying by only ±2% among control Bcl2 mice.[19] We first screened the in vivo activities of compounds such as **6b** and **6f** side by side with **6a** in a single Bcl-2 transgenic mouse with a single intraperitoneal (ip) injection at 60 and 120 μmol/kg, respectively. In agreement with all in vitro data, tested 5,5′ substituted **6a** derivatives induce significant spleen weight reduction of mice in a dose-dependent manner. Compounds **6b**, **6d**, and **6f** displayed superior in vivo activity compared to **6a** at dose of 60 μmol/kg (Figure 3A). In particular, compounds **6b** and **6f** induced more than 30−40% spleen weight reduction compared to the 20% induced by **6a**. Because the maximum spleen shrinkage would be no more than 50% in this experimental model,[19] these compounds induced near maximal (60−80%) biological activity, while **6a** induced only 40% of maximum reduction in spleen weight at the same dose. Mice treated with **6b**, **6d**, and **6f** tolerated treatment well with no observed toxicity. However, mice treated with compounds **6i**, **6l**, and **8a** at 60 μmol/kg ip, died. Nevertheless, compounds **6i** and **6l** are well tolerated when administered ip at 30 μmol/kg, resulting in significant maximal reduction of speen size of 86% ± 8.0% and 76% ± 14.0%, respectively .

To further confirm results of the single transgenic mouse experiment, we next evaluated the in vivo activity of compound **6f** in groups of seven B6-Bcl-2 transgenic mice each at a dose of 60 μmol/kg. Consistent with the single mouse experiment, compound **6f** treatment resulted in a significant (~60%) reduction of spleen weight ($P < 0.0002$) compared to the control group of seven mice (Figure 3B). All mice tolerated the treatment well, with no evident signs of toxicity. The average weight loss of mice was ~5.0% during the course of this study with compound **6f**.

To examine the therapeutic potential of compound **6a** and its derivatives (**6f** and **6i**) as a single agent against prostate cancer, the in vivo efficacy of these compounds were investigated side by side with compound **1** on the growth of PPC-1 xenograft tumors (Figure 3C). When dosed ip three times in the first week at 50 mg/kg, compound **6f** and **6a** induced strong tumor regression compared with the control group. Mice treated with **6f** and **6a** tolerated the treatment well in the first week with modest (~5%) weight loss. However, mice treated with **6i** (50 mg/kg, ip) and **1** (25 mg/kg, ip) died in the first week of this experiment. Mice were treated with **6f** and **6a** twice in the second week and once in third week at 50 mg/kg. Overall, compound **6f** displayed significant antitumor activity compared to control group, with T/C% ratios of 33% ($P < 0.001$) in PPC-1 xenograft-bearing nude mice (Figure 3C). Compound **6a** showed weaker antitumor activity compared to **6f**, with T/C% ratios of 65% in same xenograft model (Figure 3C). Mice treated with **6f** tolerated the treatment well with no observable signs of toxicity (Figure 3D). Average

body weight losses during the treatment are 6.8%, 7.1%, and 9.3% for **6f**, control, and **6a** group, respectively.

Conclusions

In summary, a series of 5,5′ substituted **6a** derivatives were synthesized and evaluated in a variety of in vitro and in vivo assays. The compound **6f** was found to bind to Bcl-X_L, Bcl-2, and Mcl-1, with IC_{50} values of 3.10, 3.12, and 2.05 μM, respectively. In a cellular assay, **6f** potently inhibited growth in cultures of the PC3, H460, H1299, and BP3 cancer cell lines, which express Bcl-X_L, Bcl-2, Mcl-1, and Bfl-1, respectively, with EC_{50} values in the single-digit micromolar to nanomolar range. Compound **6f** effectively induced apoptosis of the RS4;11 human lymphoma cell line and primary human chronic lymphocytic leukemia cells in a dose-dependent manner. Compound **6f** also displays in vivo efficacy in transgenic mice in which Bcl-2 is overexpressed in splenic B-cells. Finally, compound **6f** showed favorable in vitro ADME properties and superior in vivo efficacy as a single agent in a PPC-1 nude mouse xenograft model relative to **6a**. Considering the critical roles of antiapoptotic Bcl-2 family proteins in tumorgenesis, chemoresistance, and the potent inhibitory activity of **6f** against antiapoptotic Bcl-2 family proteins, compound **6f** represents a viable drug candidate for the development of novel apoptosis-based cancer therapies.

Experimental Section

General Synthetic Procedures. Unless otherwise indicated, all reagents and anhydrous solvents (CH_2Cl_2, THF, diethyl ether, etc.) were obtained from commercial sources and used without purification. All reactions were performed in oven-dried glassware. All reactions involving air or moisture sensitive reagents were performed under a nitrogen atmosphere. Silica gel or reverse phase chromatography was performed using prepacked silica gel or C-18 cartridges (RediSep), respectively. All final compounds were purified to >95% purity, as determined by a HPLC Breeze from Waters Co. using an Atlantis T3 3 μM 4.6 mm × 150 mm reverse phase column. Method A: The eluant was a linear gradient with a flow rate of 1 mL/min from 50% A and 50% B to 5% A and 95% B in 15 min, followed by 5 min at 100% B (solvent A, H_2O with 0.1% TFA; solvent B, ACN with 0.1% TFA). Compounds were detected at $\lambda = 254$ nm. Method B: The eluant was a linear gradient with a flow rate of 1 mL/min from 20% A and 80% B to 100% B in 15 min, followed by 5 min at 100% B (solvent A, H_2O with 0.1% TFA; solvent B, ACN with 0.1% TFA). Compounds were detected at $\lambda = 254$ nm. ^{1}H NMR spectra were recorded on Varian 300 or Bruker 600 MHz instruments. Chemical shifts are reported in ppm (δ) relative to ^{1}H (Me_4Si at 0.00 ppm). Coupling constant[11] are reported in Hz throughout. Mass spectral data were acquired on Shimadzu LCMS-2010EV for low resolution and on an Agilent ESI-TOF for high resolution.

1,1′,6,6′,7,7′-Hexahydroxy-5,5′-diisopropyl-3,3′-dimethyl-2,2′-binaphthyl-8,8′-dicarboxaldehyde (1). Compound **1** (Gossypol) is commercially available from Yixin Pharmaceutical Co. HPLC purity 99.0%, $t_R = 12.50$ min (method A).

5,5′-Diisopropyl-1,1′,6,6′,7,7′-hexamethoxy-3,3′-dimethyl-2,2′-binaphthalene (9). The compound **1** (5 g, 8.65 mmol) in 50 mL of 40% NaOH was heated under nitrogen at 90 °C for 3.5 h in the dark. The reaction mixture was cooled and poured slowly onto ice (300 mL) and concentrated H_2SO_4 (35 mL) mixture to form white precipitate. The precipitate was filtered, washed with water, and dried to afford 3.8 g of compound **2a** (95%) as a white solid. ^{1}H NMR (300 MHz, $CDCl_3$) δ 7.61 (s, 2H), 7.50 (s, 2H), 5.93 (s, 2H), 5.27 (s, 2H), 5.13 (s, 2H), 3.88 (m, 2H), 2.12 (s, 6H), 1.55 (d, $J = 5.5$ Hz, 12H). HPLC purity 99.2%, $t_R = 13.12$ min. HRMS calcd for $C_{28}H_{30}O_6$ 463.2115 (M + H), found 463.2108. The compound **2a** (3.8 g, 8.21 mmol) was dissolved into acetone (200 mL). K_2CO_3 (23.9 g, 206.7 mmol) and dimethyl sulfate (16.3 mL, 206.7 mmol) were added, and the reaction mixture was refluxed under nitrogen for 24 h. The solid was collected by filtration and washed using acetone and water and dried to yield 4.2 g of compound **9** as white solid (93%). ^{1}H NMR (300 MHz, $CDCl_3$) 7.83 (s, 2H), 7.43 (s, 2H), 3.98 (m, 8H), 3.94 (s, 6H), 3.57 (s, 6H), 2.20 (s, 6H), 1.56 (s, 12H).

5,5′-Diisopropyl-6,6′,7,7′-tetramethoxy-3,3′-dimethyl-2,2′-binaphthyl-1,1′,4,4′-tetraone (10). Periodic acid (10 g, 43.8 mmol) was added to a solution of compound **9** (0.62 g, 1.12 mmol) in 20 mL of dioxane, and the reaction mixture was stirred at 95 °C for 15 min. Crushed ice was added to quench the reaction. The solution was extracted twice with ethyl acetate, and the organic layer was washed with water, brine, and dried over $MgSO_4$. The solvent was concentrated in vacuo and the residue was purified by flash silica column chromatography to give 142 mg of compound **10** (23%) as yellow solid. ^{1}H NMR (600 MHz, CD_3OD) δ 7.56 (s, 2H), 4.31 (m, 2H), 3.97 (s, 6H), 3.94 (s, 6H), 2.03 (s, 6H), 1.40 (d, $J = 1.8$ Hz, 6H), 1.39 (d, $J = 1.8$ Hz, 6H).

6,6′,7,7′-Tetrahydroxy-5,5′-diisopropyl-3,3′-dimethyl-2,2′-binaphthyl-1,1′,4,4′-tetraone (6a). BBr_3 (0.54 mL, 1.43 g, 5.71 mmol) was added dropwise into a solution of compound **10** (260 mg, 0.48 mmol) in 10 mL of anhydrous CH_2Cl_2 at −78 °C. Stirring was continued at −78 °C for 1 h, 0 °C for 1 h, and ambient temperature for 1 h. Ice (50 g) containing 5 mL of 6 M HCl was added to the mixture and stirred for 1 h at room temperature. The aqueous layer was extracted with dichloromethane (3 × 50 mL). The combined organic layer was washed with water and brine and dried over $MgSO_4$. The solvent was concentrated in vacuo, and the residue was purified using C-18 column chromatography (H_2O/acetonitrile), followed by recrystallization from ethyl acetate/hexane to give 163 mg of compound **6a** (70%) as brown−yellow solid. ^{1}H NMR (600 MHz, CD_3OD) δ 7.31 (s, 2H), 4.32 (m, 2H), 1.88 (s, 6H), 1.42 (s, 6H), 1.40 (s, 6H). ^{13}C NMR (600 MHz, $(CD_3)_2SO$)) δ 187.10, 182.51, 150.92, 149.54, 147.60, 137.78, 137.10, 126.24, 125.00, 111.03, 27.07, 20.50, 20.35, 15.00. HPLC purity 99.5%, $t_R = 11.60$ min (method A). HRMS calcd for $C_{28}H_{26}O_8$ 491.1700 (M + H), found 491.1696.

The syntheses of compounds **3** and **4** have been previously described.[22,23]

6,6′,7,7′-Tetrahydroxy-3,3′-dimethyl-1,1′,4,4′-tetraoxo-N^5,$N^{5'}$-bis(2-phenylpropyl)-1,1′,4,4′-tetrahydro-2,2′-binaphthyl-5,5′-dicarboxamide (8a). A solution of compound **4a** (290 mg, 0.414 mmol) in 12 mL of acetone and 23 mL of acetic acid was heated on an oil bath (60−67 °C) during the addition of 18 mL of a 10% aqueous solution of ferric chloride (6.64 mmol) and for several minutes longer. The solution was cooled, and 30 mL of water was added followed by 20 mL of aqueous 20% sulfuric acid. The solution was extracted twice with diethyl ether, and the organic layer was washed with water and brine and dried over $MgSO_4$. The solvent was concentrated in vacuo, and the residue was purified by C-18 column chromatography (H_2O/acetonitrile) to give 60 mg of compound **8a** (45%) as yellow solid. ^{1}H NMR (600 MHz, CD_3OD) δ 7.42 (s, 2H), 7.34 (d, $J = 7.2$ Hz, 4H), 7.30 (t, $J_1 = J_2 = 7.2$ Hz, 4H), 7.18 (t, $J_1 = J_2 = 7.2$ Hz, 4H), 3.54 (d, $J = 7.2$ Hz, 4H), 3.22 (m, 2H), 1.91 (s, 6H), 1.39 (s, 6H), 1.38 (d, $J = 6.6$ Hz, 6H). ^{13}C NMR (600 MHz, CD_3OD) δ 184.50, 183.68, 170.44, 151.92, 150.19, 146.99, 146.55, 140.68, 129.63, 128.54, 127.53, 127.23, 126.13, 124.30, 113.14, 48.34, 40.74, 19.97, 14.50. HPLC purity 98.3%, $t_R = 5.82$ min (method A). HRMS calcd for $C_{42}H_{36}N_2O_{10}$ 729.2443 (M + H), found 729.2441.

Following above-mentioned procedure and the appropriate starting materials and reagents used; compounds **7** and **8b**−**8c** were synthesized.

6,6′,7,7′-Tetrahydroxy-3,3′-dimethyl-N^5,$N^{5'}$-bis(3-methylbenzyl)-1,1′,4,4′-tetraoxo-1,1′,4,4′-tetrahydro-2,2′-binaphthyl-5,5′-dicarboxamide (8b). Yield, 50%. ^{1}H NMR (600 MHz, CD_3OD) δ 7.44 (s, 2H), 7.39 (s, 2H), 7.29 (d, $J = 7.2$ Hz, 2H), 7.20 (t, $J_1 = 7.2$ Hz, $J_2 = 7.8$ Hz, 4H), 7.06 (d, $J = 7.8$ Hz, 2H), 4.61 (dd, $J_1 = 15$ Hz,

J_2 = 4.8 Hz, 4H), 2.35 (s, 6H), 1.91 (s, 6H). ^{13}C NMR (600 MHz, CD_3OD) δ 184.57, 183.70, 170.33, 152.01, 150.28, 147.04, 139.71, 139.24, 129.68, 129.41, 128.87, 127.33, 126.04, 126.00, 124.32, 113.21, 44.65, 21.66, 14.49. HPLC purity 99.0%, t_R = 5.53 min (method A). HRMS calcd for **$C_{40}H_{32}N_2O_{10}$** 701.2130 (M + H), found 701.2128.

***N*^{5},*N*$^{5'}$-Bis(4-ethylphenethyl)-6,6′,7,7′-tetrahydroxy-3,3′-dimethyl-1,1′,4,4′-tetraoxo-1,1′,4,4′-tetrahydro-2,2′-binaphthyl-5,5′-dicarboxamide (8c).** Yield, 52%. ^{1}H NMR (600 MHz, CD_3OD) δ 7.43 (s, 2H), 7.23 (d, J = 6.6 Hz, 4H), 7.12 (d, J = 6.6 Hz, 4H), 3.60 (m, 4H), 2.96 (t, J_1 = J_2 = 6.6 Hz, 4H), 2.50 (q, J_1 = J_2 = 6.6 Hz, 4H), 1.93 (s, 6H), 1.20 (t, J_1 = J_2 = 6.6 Hz, 6H). ^{13}C NMR (600 MHz, CD_3OD) δ 184.55, 183.68, 170.37, 151.99, 150.18, 147.01, 143.51, 140.73, 138.24, 130.09, 129.09, 127.38, 126.09, 124.31, 113.18, 43.03, 36.03, 29.68, 16.49, 14.51. HPLC purity 97.6%, t_R = 6.99 min (method A). HRMS calcd for **$C_{44}H_{40}N_2O_{10}$** 757.2756 (M + H), found 757.2745.

6,6′,7,7′-Tetrahydroxy-3,3′-dimethyl-5,5′-bis(2-phenylacetyl)-2,2′-binaphthyl-1,1′,4,4′-tetraone (7). Yield, 49%. ^{1}H NMR (600 MHz, CD_3OD) δ 7.32 (s, 2H), 7.28 (d, J = 6.0 Hz, 4H), 7.22 (t, J_1 = J_2 = 6.0 Hz, 4H), 7.15 (t, J_1 = J_2 = 6.0 Hz, 2H), 4.13 (m, 4H), 1.93 (s, 6H). ^{13}C NMR (600 MHz, CD_3OD) δ 204.02, 183.63, 181.97, 150.74, 147.30, 145.10, 139.75, 134.05, 130.14, 129.78, 127.70, 126.40, 125.69, 122.90, 111.65, 49.31, 12.84. HPLC purity 99.0%, t_R = 9.44 min (method A). HRMS calcd for **$C_{38}H_{26}O_{10}$** 643.1599 (M + H), found 643.1601.

1,1′,6,6′,7,7′-Hexamethoxy-3,3′-dimethyl-5,5′-bis(4-methylphenethyl)-2,2′-binaphthyl (15f). To a freshly prepared 4-methylbenzylmagnesium chloride (30.85 mmol) solution at room temperature was added a solution of **11** (2.0 g, 3.86 mmol) in anhydrous tetrahydrofuran (30 mL), and the reaction mixture was heated at 30 °C for 18 h. The reaction mixture was poured onto saturated ammonium chloride solution, and the aqueous layer was extracted twice with diethyl ether, washed with brine, and dried over $MgSO_4$. Filtration followed by evaporation of the ether gave yellow oil **13**. To a solution of the yellow oil **13** (1.4 g, 1.929 mmol) in 25 mL of TFA was added 3.1 mL of triethylsilane dropwise. The solution was heated at 75 °C for 1 h followed by stirring at room temperature for 18 h. The solution was concentrated in vacuo followed by silica gel column chromatography to give 660 mg compound **15f** as colorless oil (50% from **11**). ^{1}H NMR (600 MHz, $CDCl_3$) δ 7.64 (s, 2H), 7.44 (s, 2H), 7.26 (d, J = 7.8 Hz, 4H), 7.15 (d, J = 7.8 Hz, 4H), 3.99 (s, 6H), 3.94 (s, 6H), 3.60 (s, 6H), 3.37 (t, J_1 = J_2 = 8.40 Hz, 4H), 2.98 (t, J_1 = J_2 = 8.4 Hz, 4H), 2.35 (s, 6H), 2.20 (s, 6H).

3,3′-Dimethyl-5,5′-bis(4-methylphenethyl)-2,2′-binaphthyl-1,1′,-6,6′,7,7′-hexaol (2f). BBr_3 solution (2.1 mL, 5.56 g, 22.2 mmol) was added dropwise into a solution of **15f** (1.23 g, 1.76 mmol) in 60 mL of anhydrous CH_2Cl_2 at −78 °C. Stirring was continued at −78 °C for 1 h, 0 °C for 1 h, and ambient temperature for 1 h, respectively. Ice (300 g) containing 30 mL of 6 M HCl was added to the mixture and stirred for 0.5 h at room temperature. The aqueous layer was extracted with dichloromethane (3×100 mL). The combined organic layer was washed with water and brine and dried over $MgSO_4$. The solvent was concentrated in vacuo, and the residue was purified by C-18 column chromatography (H_2O/acetonitrile) to give 1.1 g of compound **2f** (90%) as white solid. Yield, 45%. ^{1}H NMR (600 MHz, CD_3OD) δ 7.45 (s, 2H), 7.34 (s, 2H), 7.20 (d, J = 7.2 Hz, 4H), 7.08 (d, J = 7.2 Hz, 4H), 3.27 (m, 4H), 2.87 (m, 4H), 2.31 (s, 6H), 2.03 (s, 6H). HPLC purity 96.6%, t_R = 17.00 min (method A). HRMS calcd for **$C_{40}H_{38}O_6$** 615.2741 (M + H), found 615.2720.

6,6′,7,7′-Tetrahydroxy-3,3′-dimethyl-5,5′-bis(4-methylphenethyl)-2,2′-binaphthyl-1,1′,4,4′-tetraone (6f). A solution of compound **2f** (1.0 g, 1.55 mmol) in 50 mL of acetone and 80 mL of acetic acid was heated on an oil bath (60−67 °C) during the addition of 68 mL of a 10% aqueous solution of ferric chloride and for several minutes longer. The solution was cooled, and 50 mL of water was added, followed by 30 mL of aqueous 20% sulfuric acid. The solution was extracted twice with diethyl ether, and the organic layer was washed with water and brine and dried over $MgSO_4$. The solvent was concentrated in vacuo, and the residue was purified by C-18 column chromatography (H_2O/acetonitrile) to give 350 mg of compound **6f** (35%) as yellow solid. ^{1}H NMR (600 MHz, CD_3OD) δ 7.40 (s, 2H), 7.22 (d, J = 7.8 Hz, 4H), 7.08 (d, J = 7.2 Hz, 4H), 3.45 (m, 4H), 2.78 (t, J_1 = 8.4 Hz, J_2 = 7.8 Hz, 4H), 2.30 (s, 6H), 1.93 (s, 6H). ^{13}C NMR (600 MHz, CD_3OD) δ 185.65, 182.87, 149.35, 148.72, 146.61, 139.47, 138.20, 134.62, 131.79, 128.32, 128.14, 126.47, 123.95, 110.50, 34.44, 28.68, 19.69, 13.36. HPLC purity 99.0%, t_R = 17.53 min (method A). HRMS calcd for **$C_{40}H_{34}O_8$** 643.2326 (M + H), found 643.2326.

Following above-mentioned procedure and the appropriate starting materials and reagents used, compounds **6b−i**, **6l** and **6m** were synthesized.

6,6′,7,7′-Tetrahydroxy-5,5′-diisobutyl-3,3′-dimethyl-2,2′-binaphthyl-1,1′,4,4′-tetraone (6b). Yield, 50%. ^{1}H NMR (600 MHz, CD_3OD) δ 7.39 (s, 2H), 3.18 (m, 4H), 1.94 (m, 2H), 1.93 (s, 6H), 0.96 (d, J = 6.0 Hz, 6H). ^{13}C NMR (600 MHz, $(CD_3)_2SO$)) δ 185.67, 182.75, 149.97, 149.53, 146.67, 138.38, 132.10, 126.65, 123.60, 111.39, 34.43, 29.18, 23.13, 23.11, 14.96. HPLC purity 96.7%, t_R = 13.68 min (method A). HRMS calcd for **$C_{30}H_{30}O_8$** 519.2013 (M + H), found 519.2012.

5,5′-Bis(cyclopentylmethyl)-6,6′,7,7′-tetrahydroxy-3,3′-dimethyl-2,2′-binaphthyl-1,1′,4,4′-tetraone (6c). Yield, 40%. ^{1}H NMR (600 MHz, $(CD_3)_2SO$) δ 10.99 (s, br, 2H), 9.54 (s, br, 2H), 7.34 (s, 2H), 3.23 (dd, J_1 = 7.2 Hz, J_2 = 4.8 Hz, 2H), 3.15 (dd, J_1 = 7.2 Hz, J_2 = 4.8 Hz, 2H), 2.10 (m, 2H), 1.87 (s, 6H), 1.61 (m, 8H), 1.45 (m, 4H), 1.26 (m, 4H). ^{13}C NMR (600 MHz, $(CD_3)_2SO$)) δ 185.25, 182.29, 149.36, 149.00, 146.23, 137.95, 132.26, 126.19, 123.05, 110.84, 40.26, 32.00, 30.65, 24.50, 14.52. HPLC purity 99.0%, t_R = 16.80 min (method A). HRMS calcd for **$C_{34}H_{34}O_8$** 571.2326 (M + H), found 571.2323.

5,5′-Bis(2-cyclohexylethyl)-6,6′,7,7′-tetrahydroxy-3,3′-dimethyl-2,2′-binaphthyl-1,1′,4,4′-tetraone (6d). Yield, 50%. ^{1}H NMR (600 MHz, $(CD_3)_2SO$) δ 10.88 (s, br, 2H), 9.51 (s, br, 2H), 7.30 (s, 2H), 3.08 (m, 4H), 1.85 (s, 6H), 1.80 (d, J = 12.0 Hz, 4H), 1.68 (d, J = 12.6 Hz, 4H), 1.61 (d, J = 11.4 Hz, 2H), 1.35 (m, 6H), 1.23 (q, J_1 = 24.6 Hz, J_2 = 12.6 Hz, 4H), 1.16 (m, 2H), 0.96 (m, 4H). ^{13}C NMR (600 MHz, $(CD_3)_2SO$)) δ 185.20, 182.22, 148.95, 148.85, 146.16, 138.00, 133.20, 125.96, 123.03, 110.72, 38.02, 36.26, 32.87, 26.32, 25.91, 23.93, 14.44. HPLC purity 98.5%, t_R = 14.76 min (method B). HRMS calcd for **$C_{38}H_{42}O_8$** 627.2952 (M + H), found 627.2952.

6,6′,7,7′-Tetrahydroxy-3,3′-dimethyl-5,5′-diphenethyl-2,2′-binaphthyl-1,1′,4,4′-tetraone (6e). Yield, 38%. ^{1}H NMR (600 MHz, CD_3OD) δ 7.41 (s, 2H), 7.36 (d, J = 7.8 Hz, 4H), 7.28 (t, J_1 = 7.8 Hz, J_2 = 7.2 Hz, 4H), 7.16 (t, J_1 = 7.8 Hz, J_2 = 7.2 Hz, 2H), 3.47 (m, 4H), 2.84 (t, J_1 = 8.4 Hz, J_2 = 7.8 Hz, 4H), 1.95 (s, 6H). HPLC purity 99.0%, t_R = 15.48 min (method A). HRMS calcd for **$C_{38}H_{30}O_8$** 615.2013 (M + H), found 615.2015.

6,6′,7,7′-Tetrahydroxy-3,3′-dimethyl-5,5′-bis(3-phenylpropyl)-2,2′-binaphthyl-1,1′,4,4′-tetraone (6g). Yield, 42%. ^{1}H NMR (600 MHz, CD_3OD) δ 7.39 (s, 2H), 7.26 (m, 8H), 7.14 (m, 2H), 3.27 (m, 4H), 2.81 (t, J_1 = J_2 = 7.8 Hz, 4H), 1.97 (s, 6H), 1.90 (p, J_1 = J_2 = 7.8 Hz, 4H). ^{13}C NMR (600 MHz, CD_3OD) δ 185.90, 183.4, 149.40, 148.80, 146.70, 142.80, 138.22, 132.54, 127.96, 127.75, 126.61, 125.11, 123.67, 110.42, 36.15, 30.73, 26.21. HPLC purity 98.0%, t_R = 16.20 min (method A). HRMS calcd for **$C_{40}H_{34}O_8$** 643.2326 (M + H), found 643.2334.

6,6′,7,7′-Tetrahydroxy-3,3′-dimethyl-5,5′-bis(3-methyl-3-phenylbutyl)-2,2′-binaphthyl-1,1′,4,4′-tetraone (6h). Yield, 50%. ^{1}H NMR (600 MHz, CD_3OD) δ 7.52 (d, J = 7.8 Hz, 4H), 7.36 (s, 2H), 7.32 (t, J_1 = J_2 = 7.8 Hz, 4H), 7.16 (t, J_1 = 7.2 Hz, J_2 = 7.8 Hz, 2H), 3.04 (t, J_1 = 7.8 Hz, J_2 = 8.4 Hz, 4H), 1.96 (s, 6H), 1.91 (m, 4H), 1.47 (s, 12H). HPLC purity 98.0%, t_R = 13.5 min (method B). ^{13}C NMR (600 MHz, CD_3OD) δ 185.36, 182.93, 149.38, 148.47, 146.58, 138.18, 133.24, 131.96, 127.47, 126.47, 125.66, 124.84, 123.69, 110.29, 42.15, 37.51, 35.48, 28.19, 22.01. HRMS calcd for **$C_{44}H_{42}O_8$** 699.2952 (M + H), found 699.2964.

5,5′-Dibenzyl-6,6′,7,7′-tetrahydroxy-3,3′-dimethyl-2,2′-binaphthyl-1,1′,4,4′-tetraone (6i). Yield, 55%. ^{1}H NMR (600 MHz, CD_3OD) δ 7.44 (s, 2H), 7.22 (d, J = 7.2 Hz, 4H), 7.17 (t, J_1 = 7.2 Hz, J_2 = 7.8 Hz, 4H), 7.17 (t, J_1 = 7.2 Hz, J_2 = 7.8 Hz, 2H), 4.63 (q, J_1 = 11.4 Hz, J_2 = 14.4 Hz, 4H), 1.86 (s, 6H). ^{13}C NMR (600 MHz, $(CD_3)_2SO$)) δ 185.38, 182.54, 149.94, 149.77, 146.53, 140.89, 138.49, 130.01, 128.60, 128.33, 126.45, 125.76, 123.69, 111.68, 31.68, 14.77. HPLC purity 99.6%, t_R = 12.12 min (method A). HRMS calcd for $\mathbf{C_{36}H_{26}O_8}$ 587.1700 (M + H), found 587.1710.

5,5′-Bis(4-chlorobenzyl)-6,6′,7,7′′-tetrahydroxy-3,3′′-dimethyl-2,2′-binaphthyl-1,1′,4,4′-tetraone (6l). Yield, 60%. ^{1}H NMR (600 MHz, CD_3OD) δ 7.45 (s, 2H), 7.22 (d, J = 6.4 Hz, 4H), 7.18 (d, J = 6.4 Hz, 4H), 4.59 (dd, J_1 = 13.8 Hz, J_2 = 26.4 Hz, 4H), 1.85 (s, 6H). HPLC purity 99.0%, t_R = 14.88 min (method A). HRMS calcd for $\mathbf{C_{40}H_{32}F_2O_8}$ 655.0921 (M + H), found 655.0931.

5,5′-Bis(biphenyl-4-ylmethyl)-6,6′,7,7′-tetrahydroxy-3,3′-dimethyl-2,2′-binaphthyl-1,1′,4,4′-tetraone (6m). Yield, 52%. ^{1}H NMR (600 MHz, CD_3OD) δ 7.55 (d, J = 7.2 Hz, 4H), 7.44 (d, J = 7.8 Hz, 6H), 7.38 (t, J_1 = 7.2 Hz, J_2 = 7.8 Hz, 4H), 7.30 (d, J = 7.8 Hz, 4H), 7.27 (t, J_1 = 7.2 Hz, J_2 = 6.6 Hz, 2H), 4.59 (dd, J_1 = 13.8 Hz, J_2 = 27.0 Hz, 4H), 1.88 (s, 6H). HPLC purity 99.0%, t_R = 16.96 min (method A). HRMS calcd for $\mathbf{C_{40}H_{32}F_2O_8}$ 739.2326 (M + H), found 739.2329.

6,6′,7,7′-Tetrahydroxy-3,3′-dimethyl-5,5′-bis(4-(trifluoromethoxy)phenethyl)-2,2′-binaphthyl-1,1′,4,4′-tetraone (6j). To a solution of **3j** (100 mg, 0.13 mmol) in 25 mL of ethanol and 1 mL of acetic acid at room temperature under H_2, 10% palladium on carbon (0.10 g) was added and stirred overnight. The solution was extracted twice with diethyl ether, and the organic layer was washed with water and brine and dried over $MgSO_4$. The solvent was concentrated in vacuo, and the crude residue (**2j**) was dissolved in 5 mL of acetone and 8 mL of acetic acid and was heated in an oil bath (60−67 °C) during the addition of 7 mL of a 10% aqueous solution of ferric chloride and then for several minutes longer. The solution was cooled, and 5 mL of water was added, followed by 3 mL of aqueous 20% sulfuric acid. The solution was extracted twice with diethyl ether, and the organic layer was washed with water and brine and dried over $MgSO_4$. The solvent was concentrated in vacuo, and the residue was purified by C-18 column chromatography (H_2O/acetonitrile) to give 30 mg of compound **6j** (30%) as yellow−brown solid. ^{1}H NMR (600 MHz, CD_3OD) δ 7.48 (d, J = 7.8 Hz, 4H), 7.42 (s, 2H), 7.20 (d, J = 7.8 Hz, 4H), 3.48 (m, 4H), 2.88 (t, J_1 = 8.4 Hz, J_2 = 7.2 Hz, 4H), 1.95 (s, 6H). HPLC purity 97.0%, t_R = 11.67 min (method B). HRMS calcd for $\mathbf{C_{40}H_{28}F_6O_{10}}$ 783.1659 (M + H), found 783.1659.

Following above-mentioned procedure and the appropriate starting materials and reagents used, compound **6k** was synthesized.

5,5′-Bis(3-(4-fluorophenyl)propyl)-6,6′,7,7′-tetrahydroxy-3,3′-dimethyl-2,2′-binaphthyl-1,1′,4,4′-tetraone (6k). Yield, 45%. ^{1}H NMR (600 MHz, CD_3OD) δ 7.37 (s, 2H), 7.24 (m, 4H), 6.97 (m, 4H), 3.26 (m, 4H), 2.78 (t, J_1 = 7.2 Hz, J_2 = 7.8 Hz, 4H), 1.94 (s, 6H), 1.90 (m, 4H). HPLC purity 96.5%, t_R = 8.76 min (method B). HRMS calcd for $\mathbf{C_{40}H_{32}F_2O_8}$ 679.2138 (M + H), found 679.2150.

Molecular Modeling. Molecular modeling studies were conducted on a Linux workstation and a 64 3.2-GHz CPUs Linux cluster. Docking studies were performed using the crystal structure of Bcl-2 in complex with a benzothiazole BH3 mimetic ligand (Protein Data Bank code 1YSW)[33,34] The ligand was extracted from the protein structure and was used to define the binding site for small molecules. Compound **6a** and its derivatives were docked into the Bcl-2 protein by the GOLD[51] docking program using ChemScore[52] as the scoring function. The active site radius was set at 10 Å, and 10 GA solutions were generated for each molecule. The GA docking procedure in GOLD[51] allowed the small molecules to flexibly explore the best binding conformations, whereas the protein structure was static. The protein surface was prepared with the program MOLCAD[53] as implemented in Sybyl (Tripos, St. Louis) and was used to analyze the binding poses for studied small molecules.

Fluorescence Polarization Assays (FPAs). A Bak BH3 peptide (F-BakBH3) (GQVGRQLAIIGDDINR) was labeled at the N-terminus with fluorescein isothiocyanate (FITC) (Molecular Probes) and purified by HPLC. For competitive binding assays, 100 nM GST−Bcl-X_L ΔTM protein was preincubated with the tested compound at varying concentrations in 47.5 μL PBS (pH = 7.4) in 96-well black plates at room temperature for 10 min, and then 2.5 μL of 100 nM FITC-labeled Bak BH3 peptide was added to produce a final volume of 50 μL. The wild-type and mutant Bak BH3 peptides were included in each assay plate as positive and negative controls, respectively. After 30 min of incubation at room temperature, the polarization values in millipolarization units[54] were measured at excitation/emission wavelengths of 480/535 nm with a multilabel plate reader (PerkinElmer). IC_{50} was determined by fitting the experimental data to a sigmoidal dose−response nonlinear regression model (SigmaPlot 10.0.1, Systat Software, Inc., San Jose, CA, USA). Data reported are the mean of three independent experiments ± standard error (SE). Performance of Bcl-2 and Mcl-1 FPA are similar. Briefly, 50 nM of GST−Bcl-2 or −Mcl-1 were incubated with various concentrations of compound **6a** or its 5,5′ substituted derivatives for 2 min, and then 15 nM FITC-conjugated-Bim BH3 peptide[55] was added in PBS buffer. Fluorescence polarization was measured after 10 min.

Cell Viability and Apoptosis Assays. The activity of the compounds against human cancer cell lines (PC3, H460, H1299) were assessed by using the ATP-LITE assay (PerkinElmer). All cells were seeded in either 12F2 or RPMI1640 medium with 5 mM L-glutamine supplemented with 5% fetal bovine serum (Mediatech Inc.), penicillin, and streptomycin (Omega). For maintenance, cells were cultured in 5% FBS. Cells were plated into 96-well plates at varying initial densities depending on doubling time. H460 and H1299 plated at 2000 cells/well and PC3 at 3000 cells/well. Compounds were diluted to final concentrations with 0.1% DMSO. Prior to dispensing compounds onto cells, fresh 5% media was placed into wells. Administration of compounds occurred 24 h after seeding into the fresh media. Cell viability was evaluated using ATP-LITE reagent (PerkinElmer) after 72 h of treatment. Data were normalized to the DMSO control-treated cells using Prism version 5.01 (Graphpad Software).

The apoptotic activity of the compounds against RS4;11, BP3, and primary CLL cells was assessed by staining with Annexin V-FITC and propidium iodide (PI). Cells were cultured in RPMI1640 medium (Mediatech Inc., Herndon, VA 20171, USA) containing 10% fetal bovine serum (Mediatech Inc.) and penicillin/streptomycin (Mediatech Inc.). Cells were cultured with various concentrations of 5,5′ substituted **6a** derivatives for 1 day. The percentage of viable cells was determined by FITC-Annexin V- and propidium iodide (PI)-labeling, using an Apoptosis Detection kit (BioVision Inc.) and analyzing stained cells by flow cytometry (FACSort; Bectin-Dickinson, Inc., Mountain View, CA, USA). Cells that were annexin-V-negative and PI-negative were considered viable.

Bcl-2 Transgenic Mice Studies. Transgenic mice expressing Bcl-2 have been described as the B6 line.[56] The *BCL-2* transgene represents a minigene version of a t(14;18) translocation in which the human *BCL-2* gene is fused with the immunoglobulin heavy-chain (IgH) locus and associated IgH enhancer. The transgene was propagated on the Balb/c background. These mice develop polyclonal B-cell hyperplasia with asynchronous transformation to monoclonal aggressive lymphomas beginning at approximately 6 months of age, with approximately 90% of mice undergoing transformation by the age of 12−24 months. All animals used here had not yet developed aggressive lymphoma. Compounds dissolved in 500 μL of solution (ethanol: Cremophor EL:saline = 10:10:80) were injected intraperitoneally to age- and sex-matched B6Bcl2 mouse, while control mice

were injected intraperitoneally with 500 μL of the same formulation without compound. After 24 h, B6Bcl2 mice were sacrificed by intraperitoneal injection of a lethal dose of Avertin. Spleen was removed and weighed. The spleen weight of mice is used as an end-point for assessing activity, as we determined that spleen weight is highly consistent in age- and sex-matched Bcl-2-transgenic mice in preliminary studies.[20] Variability of spleen weight was within ±2% among control-treated age-matched, sex-matched B6Bcl2 mice.

Tumor Xenograft Studies. Female 6-week-old nude mice were purchased from Charles River Laboratories. PCC-1 cells (5×10^6) suspended in 0.2 mL of PBS were injected subcutaneously into a flank region of each nude mouse. Tumor bearing mice were size matched (200 mm^3) into treatment and control group, ear tagged, and monitored individually. Tumor volume was measured two to three times weekly by digital calipers (volume = (length × $width^2$)/2). All studies use six mice per group. Compounds dissolved in 500 μL of solvent (ethanol:Cremophor EL: saline = 10:10:80) were injected intraperitoneally (ip) into tumor-beraing mice. Control mice received saline. The injections were given three times in the first week, twice in second week, and once in the third week, and a total of six injections were administered during the experiment. When all tumors of the control group exceed 2000 mm^3 in volume, the animal experiment was terminated. Tumor growth inhibition ratios (T/C %) were calculated by dividing the average tumor volume in the treatment group by the average tumor volume in the control group.

Acknowledgment. We thank NIH (grants CA113318 and CA149668 to M.P. and J.C.R.) for financial support.

Supporting Information Available: Experimental section including information on chemical data for compounds **15b**−**i** and **2b**−**2m**, NMR experiments, isothermal titration calorimetry assays, in vitro ADME studies, and in vivo mice studies. This material is available free of charge via the Internet at http://pubs.acs.org.

References

(1) Vaux, D. L.; Korsmeyer, S. J. Cell death in development. *Cell* **1999**, *96*, 245–254.
(2) Reed, J. C. Dysregulation of apoptosis in cancer. *J. Clin. Oncol.* **1999**, *17*, 2941–2953.
(3) Johnstone, R. W.; Ruefli, A. A.; Lowe, S. W. Apoptosis: a link between cancer genetics and chemotherapy. *Cell* **2002**, *108*, 153–164.
(4) Reed, J. C. Apoptosis-based therapies. *Nature Rev. Drug Discovery* **2002**, *1*, 111–121.
(5) Reed, J. C. Molecular biology of chronic lymphocytic leukemia: implications for therapy. *Semin. Hematol.* **1998**, *35*, 3–13.
(6) Adams, J. M.; Cory, S. The Bcl-2 protein family: arbiters of cell survival. *Science* **1998**, *281*, 1322–1326.
(7) Gross, A.; McDonnell, J. M.; Korsmeyer, S. J. BCL-2 family members and the mitochondria in apoptosis. *Genes Dev.* **1999**, *13*, 1899–1911.
(8) Reed, J. C. Bcl-2 family proteins. *Oncogene* **1998**, *17*, 3225–3236.
(9) Wang, J. L.; Liu, D.; Zhang, Z. J.; Shan, S.; Han, X.; Srinivasula, S. M.; Croce, C. M.; Alnemri, E. S.; Huang, Z. Structure-based discovery of an organic compound that binds Bcl-2 protein and induces apoptosis of tumor cells. *Proc. Natl. Acad. Sci. U.S.A.* **2000**, *97*, 7124–7129.
(10) Degterev, A.; Lugovskoy, A.; Cardone, M.; Mulley, B.; Wagner, G.; Mitchison, T.; Yuan, J. Identification of small-molecule inhibitors of interaction between the BH3 domain and Bcl-xL. *Nature Cell Biol.* **2001**, *3*, 173–182.
(11) Reed, J. C. Bcl-2 family proteins: strategies for overcoming chemoresistance in cancer. *Adv. Pharmacol.* **1997**, *41*, 501–532.
(12) Kitada, S.; Leone, M.; Sareth, S.; Zhai, D.; Reed, J. C.; Pellecchia, M. Discovery, characterization, and structure−activity relationships studies of proapoptotic polyphenols targeting B-cell lymphocyte/leukemia-2 proteins. *J. Med. Chem.* **2003**, *46*, 4259–4264.
(13) Zhang, M.; Liu, H.; Guo, R.; Ling, Y.; Wu, X.; Li, B.; Roller, P. P.; Wang, S.; Yang, D. Molecular mechanism of gossypol-induced cell growth inhibition and cell death of HT-29 human colon carcinoma cells. *Biochem. Pharmacol.* **2003**, *66*, 93–103.
(14) Wang, S.; Yang, D. Small Molecular Antagonists of Bcl-2 family proteins. U.S. Patent 2003008924, 2002.
(15) Wang, G.; Nikolovska-Coleska, Z.; Yang, C.-Y.; Wang, R.; Tang, G.; Guo, J.; Shangary, S.; Qiu, S.; Gao, W.; Yang, D.; Meagher, J.; Stuckey, J.; Krajewski, K.; Jiang, S.; Roller, P. P.; Abaan, H. O.; Tomita, Y.; Wang, S. Structure-based design of potent small-molecule inhibitors of anti-apoptotic Bcl-2 proteins. *J. Med. Chem.* **2006**, *49*, 6139–6142.
(16) Mohammad, R. M.; Wang, S.; Aboukameel, A.; Chen, B.; Wu, X.; Chen, J.; Al-Katib, A. Preclinical studies of a nonpeptidic small-molecule inhibitor of Bcl-2 and Bcl-X(L) [(−)-gossypol] against diffuse large cell lymphoma. *Mol. Cancer Ther.* **2005**, *4*, 13–21.
(17) Meng, Y.; Tang, W.; Dai, Y.; Wu, X.; Liu, M.; Ji, Q.; Ji, M.; Pienta, K.; Lawrence, T.; Xu, L. Natural BH3 mimetic (−)-gossypol chemosensitizes human prostate cancer via Bcl-xL inhibition accompanied by increase of Puma and Noxa. *Mol. Cancer Ther.* **2008**, *7*, 2192–2202.
(18) Becattini, B.; Kitada, S.; Leone, M.; Monosov, E.; Chandler, S.; Zhai, D.; Kipps, T. J.; Reed, J. C.; Pellecchia, M. Rational design and real time, in-cell detection of the proapoptotic activity of a novel compound targeting Bcl-X(L). *Chem. Biol.* **2004**, *11*, 389–395.
(19) Kitada, S.; Kress, C. L.; Krajewska, M.; Jia, L.; Pellecchia, M.; Reed, J. C. Bcl-2 antagonist apogossypol (NSC736630) displays single-agent activity in Bcl-2-transge3nic mice and has superior efficacy with less toxicity compared with gossypol (NSC19048). *Blood* **2008**, *111*, 3211–3219.
(20) Coward, L.; Gorman, G.; Noker, P.; Kerstner-Wood, C.; Pellecchia, M.; Reed, J. C.; Jia, L. Quantitative determination of apogossypol, a pro-apoptotic analog of gossypol, in mouse plasma using LC/MS/MS. *J. Pharm. Biomed. Anal.* **2006**, *42*, 581–586.
(21) Wei, J.; Rega, M. F.; Kitada, S.; Yuan, H.; Zhai, D.; Risbood, P.; Seltzman, H. H.; Twine, C. E.; Reed, J. C.; Pellecchia, M. Synthesis and evaluation of Apogossypol atropisomers as potential Bcl-xL antagonists. *Cancer Lett.* **2009**, *273*, 107–113.
(22) Wei, J.; Kitada, S.; Rega, M. F.; Emdadi, A.; Yuan, H.; Cellitti, J.; Stebbins, J. L.; Zhai, D.; Sun, J.; Yang, L.; Dahl, R.; Zhang, Z.; Wu, B.; Wang, S.; Reed, T. A.; Lawrence, N.; Sebti, S.; Reed, J. C.; Pellecchia, M. Apogossypol derivatives as antagonists of antiapoptotic Bcl-2 family proteins. *Mol. Cancer Ther.* **2009**, *8*, 904–913.
(23) Wei, J.; Kitada, S.; Rega, M. F.; Stebbins, J. L.; Zhai, D.; Cellitti, J.; Yuan, H.; Emdadi, A.; Dahl, R.; Zhang, Z.; Yang, L.; Reed, J. C.; Pellecchia, M. Apogossypol derivatives as pan-active inhibitors of antiapoptotic B-cell lymphoma/leukemia-2 (Bcl-2) family proteins. *J. Med. Chem.* **2009**, *52*, 4511–4523.
(24) Wei, J.; Stebbins, J. L.; Kitada, S.; Dash, R.; Placzek, W.; Rega, M. F.; Wu, B.; Cellitti, J.; Zhai, D.; Yang, L.; Dahl, R.; Fisher, P. B.; Reed, J. C.; Pellecchia, M. BI-97C1, an optically pure Apogossypol derivative as pan-active inhibitor of antiapoptotic B-cell lymphoma/leukemia-2 (Bcl-2) family proteins. *J. Med. Chem.* **2010**, *53*, 4166–4176.
(25) Shelley, M. D.; Hartley, L.; Fish, R. G.; Groundwater, P.; Morgan, J. J.; Mort, D.; Mason, M.; Evans, A. Stereospecific cytotoxic effects of gossypol enantiomers and gossypolone in tumour cell lines. *Cancer Lett.* **1999**, *135*, 171–180.
(26) Flack, M. R.; Knazek, R.; Reidenberg, M. Gossypolone for the treatment of cancer. U.S. Patent 40862. **2009**.
(27) Wang, S.; Nikolovska-Coleska, Z.; Yang, C.-Y.; Chen, J. Apogossypolone and the uses thereof. PCT Int. Appl. WO 2006050447 A2 20060511, 2006.
(28) Sun, J.; Li, Z.-M.; Hu, Z.-Y.; Zeng, Z.-L.; Yang, D.-J.; Jiang, W.-Q. Apogossypolone inhibits cell growth by inducing cell cycle arrest in U937 cells. *Oncol. Rep.* **2009**, *22*, 193–198.
(29) Lin, J.; Wu, Y.-J.; Yang, D.-J.; Zhao, Y.-Q. Effect of apogossypolone on induction apoptosis in multiple myeloma cells and its mechanisms. *Zhongguo Shiyan Xueyexue Zazhi* **2009**, *17*, 92–98.
(30) Arnold, A. A.; Aboukameel, A.; Chen, J.; Yang, D.; Wang, S.; Al-Katib, A.; Mohammad, R. M. Preclinical Studies of Apogossypolone: A New Nonpeptidic Pan Small-Molecule Inhibitor of Bcl-2, Bcl-XL and Mcl-1 Proteins in Follicular Small Cleaved Cell Lymphoma Model. *Mol. Cancer* **2008**, *7*, 20.
(31) Mi, J. X.; Wang, G. F.; Wang, H. B.; Sun, X. Q.; Ni, X. Y.; Zhang, X. W.; Tang, J. M.; Yang, D. J. Synergistic antitumoral activity and induction of apoptosis by novel pan Bcl-2 proteins inhibitor apogossypolone with adriamycin in human hepatocellular carcinoma. *Acta Pharmacol. Sin.* **2008**, *29*, 1467–1477.
(32) Hu, Z. Y.; Zhu, X. F.; Zhong, Z. D.; Sun, J.; Wang, J.; Yang, D.; Zeng, Y. X. ApoG2, a novel inhibitor of antiapoptotic Bcl-2 family proteins, induces apoptosis and suppresses tumor growth

in nasopharyngeal carcinoma xenografts. *Int. J. Cancer* **2008**, *123*, 2418–2429.
(33) Oltersdorf, T.; Elmore, S. W.; Shoemaker, A. R.; Armstrong, R. C.; Augeri, D. J.; Belli, B. A.; Bruncko, M.; Deckwerth, T. L.; Dinges, J.; Hajduk, P. J.; Joseph, M. K.; Kitada, S.; Korsmeyer, S. J.; Kunzer, A. R.; Letai, A.; Li, C.; Mitten, M. J.; Nettesheim, D. G.; Ng, S.; Nimmer, P. M.; O'Connor, J. M.; Oleksijew, A.; Petros, A. M.; Reed, J. C.; Shen, W.; Tahir, S. K.; Thompson, C. B.; Tomaselli, K. J.; Wang, B.; Wendt, M. D.; Zhang, H.; Fesik, S. W.; Rosenberg, S. H. An inhibitor of Bcl-2 family proteins induces regression of solid tumours. *Nature* **2005**, *435*, 677–681.
(34) Bruncko, M.; Oost, T. K.; Belli, B. A.; Ding, H.; Joseph, M. K.; Kunzer, A.; Martineau, D.; McClellan, W. J.; Mitten, M.; Ng, S. C.; Nimmer, P. M.; Oltersdorf, T.; Park, C. M.; Petros, A. M.; Shoemaker, A. R.; Song, X.; Wang, X.; Wendt, M. D.; Zhang, H.; Fesik, S. W.; Rosenberg, S. H.; Elmore, S. W. Studies leading to potent, dual inhibitors of Bcl-2 and Bcl-xL. *J. Med. Chem.* **2007**, *50*, 641–662.
(35) Adams, R.; Butterbaugh, D. J. Structure of Gossypol. X. Apogossypol and its Degradation Products. *J. Am. Chem. Soc.* **1938**, *60*, 2174–2180.
(36) Meltzer, P. C.; Bickford, H. P.; Lambert, G. J. A Regioselective Route to Gossypol Analogues: The Synthesis of Gossypol and 5,5′-Didesisopropyl-5,5′-diethylgossypol. *J. Org. Chem.* **1985**, *50*, 3121–3124.
(37) Yamanoi, Y.; Nishihara, H. Direct and selective arylation of tertiary silanes with rhodium catalyst. *J. Org. Chem.* **2008**, *73*, 6671–6678.
(38) Royer, R. E.; Deck, L. M.; Vander Jagt, T. J.; Martinez, F. J.; Mills, R. G.; Young, S. A.; Vander Jagt, D. L. Synthesis and anti-HIV activity of 1,1′-dideoxygossypol and related compounds. *J. Med. Chem.* **1995**, *38*, 2427–2432.
(39) Du, Y.; Liu, R.; Linn, G.; Zhao, K. Synthesis of *N*-substituted indole derivatives via PIFA-mediated intramolecular cyclization. *Org. Lett.* **2006**, *8*, 5919–5922.
(40) Islam, I.; Skibo, E. B.; Dorr, R. T.; Alberts, D. S. Structure−activity studies of antitumor agents based on pyrrolo[1,2-*a*]benzimidazoles: new reductive alkylating DNA cleaving agents. *J. Med. Chem.* **1991**, *34*, 2954–2961.
(41) Dao, V. T.; Gaspard, C.; Mayer, M.; Werner, G. H.; Nguyen, S. N.; Michelot, R. J. Synthesis and cytotoxicity of gossypol related compounds. *Eur. J. Med. Chem.* **2000**, *35*, 805–813.
(42) Tang, G.; Ding, K.; Nikolovska-Coleska, Z.; Yang, C. Y.; Qiu, S.; Shangary, S.; Wang, R.; Guo, J.; Gao, W.; Meagher, J.; Stuckey, J.; Krajewski, K.; Jiang, S.; Roller, P. P.; Wang, S. Structure-based design of flavonoid compounds as a new class of small-molecule inhibitors of the anti-apoptotic Bcl-2 proteins. *J. Med. Chem.* **2007**, *50*, 3163–3166.
(43) Sakamoto, K.; Miyoshi, H.; Takegami, K.; Mogi, T.; Anraku, Y.; Iwamura, H. Probing substrate binding site of the *Escherichia coli* quinol oxidases using synthetic ubiquinol analogues. *J. Biol. Chem.* **1996**, *271*, 29897–29902.
(44) Rega, M. F.; Leone, M.; Jung, D.; Cotton, N. J.; Stebbins, J. L.; Pellecchia, M. Structure-based discovery of a new class of Bcl-xL antagonists. *Bioorg. Chem.* **2007**, *35*, 344–353.
(45) Wesarg, E.; Hoffarth, S.; Wiewrodt, R.; Kroll, M.; Biesterfeld, S.; Huber, C.; Schuler, M. Targeting BCL-2 family proteins to overcome drug resistance in non-small cell lung cancer. *Int. J. Cancer* **2007**, *121*, 2387–2394.
(46) Brien, G.; Trescol-Biemont, M. C.; Bonnefoy-Berard, N. Down-regulation of Bfl-1 protein expression sensitizes malignant B cells to apoptosis. *Oncogene* **2007**, *26*, 5828–5832.
(47) Li, J.; Viallet, J.; Haura, E. B. A small molecule pan-Bcl-2 family inhibitor, GX15-070, induces apoptosis and enhances cisplatin-induced apoptosis in non-small cell lung cancer cells. *Cancer Chemother. Pharmacol.* **2008**, *61*, 525–534.
(48) Voortman, J.; Checinska, A.; Giaccone, G.; Rodriguez, J. A.; Kruyt, F. A. Bortezomib, but not cisplatin, induces mitochondria-dependent apoptosis accompanied by up-regulation of noxa in the non-small cell lung cancer cell line NCI-H460. *Mol. Cancer Ther.* **2007**, *6*, 1046–1053.
(49) Ferreira, C. G.; Span, S. W.; Peters, G. J.; Kruyt, F. A.; Giaccone, G. Chemotherapy triggers apoptosis in a caspase-8-dependent and mitochondria-controlled manner in the non-small cell lung cancer cell line NCI-H460. *Cancer Res.* **2000**, *60*, 7133–7141.
(50) Cory, S.; Adams, J. M. Killing cancer cells by flipping the Bcl-2/Bax switch. *Cancer Cell* **2005**, *8*, 5–6.
(51) Jones, G.; Willett, P.; Glen, R. C.; Leach, A. R.; Taylor, R. Development and validation of a genetic algorithm for flexible docking. *J. Mol. Biol.* **1997**, *267*, 727–748.
(52) Eldridge, M. D.; Murray, C. W.; Auton, T. R.; Paolini, G. V.; Mee, R. P. Empirical scoring functions: I. The development of a fast empirical scoring function to estimate the binding affinity of ligands in receptor complexes. *J. Comput.-Aided Mol. Des.* **1997**, *11*, 425–445.
(53) Teschner, M.; Henn, C.; Vollhardt, H.; Reiling, S.; Brickmann, J. Texture mapping: a new tool for molecular graphics. *J. Mol. Graphics* **1994**, *12*, 98–105.
(54) Sattler, M.; Liang, H.; Nettesheim, D.; Meadows, R. P.; Harlan, J. E.; Eberstadt, M.; Yoon, H. S.; Shuker, S. B.; Chang, B. S.; Minn, A. J.; Thompson, C. B.; Fesik, S. W. Structure of Bcl-xL-Bak peptide complex: recognition between regulators of apoptosis. *Science* **1997**, *275*, 983–986.
(55) Ramjaun, A. R.; Tomlinson, S.; Eddaoudi, A.; Downward, J. Upregulation of two BH3-only proteins, Bmf and Bim, during TGF beta-induced apoptosis. *Oncogene* **2007**, *26*, 970–981.
(56) Katsumata, M.; Siegel, R. M.; Louie, D. C.; Miyashita, T.; Tsujimoto, Y.; Nowell, P. C.; Greene, M. I.; Reed, J. C. Differential effects of Bcl-2 on T and B cells in transgenic mice. *Proc. Natl. Acad. Sci. U.S.A.* **1992**, *89*, 11376–11380.